**Development of a Powered Ankle Exoskeleton**

*Lorenzo Shaikewitz*

*Mentors: Aaron Ames and Maegan Tucker*

**Table of Contents**

## 1. Abstract

Powered exoskeletons can enhance the human ability to carry load, improve metabolic efficiency, and help the injured to a quick recovery. However, they rely on control algorithms that are difficult to test on systems with many degrees of freedom. We designed an autonomous ankle exoskeleton to reduce the metabolic cost of walking and provide a one-degree-of-freedom platform for controls testing. The lightweight device actuates two moment arms attached to the foot to generate a mechanical torque during the transition from stance to swing in the walking gait. With its modular design, electronics can be concentrated at the waist to maximize efficiency or at the shin to minimize complexity. Basic control simulations and calculations show the exoskeleton can apply torques comparable to normal biological torque, making use of a sleek angled strut design to redirect forces and maximize user comfort. Once constructed, this device will provide a platform for complex controls to optimize its own function and aid in the development of larger exoskeletons.

## 2. Introduction and Background

Powered exoskeletons provide a promising means to increase the limits of human activity and aid in the swift recovery from injury[1,2]. Over the last two decades numerous exoskeletons have been developed, with varying degrees of effectiveness and increasingly complex control[3,4]. Their designs range from full-body exoskeletons that make walking easier for those with spinal cord injuries[1], to smaller scale leg or hip exoskeletons designed to serve in military applications[2,5].

Each of these exoskeletons use different, specialized control systems to provide meaningful assistance. This control often benefits from refinement on simpler systems that only assist with a single degree of freedom. Numerous labs working on larger devices have developed small ankle exoskeletons to improve their control, but many cannot operate without tethering[6] or in many different walking gaits[7].

We developed a stand-alone powered ankle exoskeleton to test new methods of control and provide meaningful assistance while walking at many speeds. The high level exoskeleton design is based on a previous design by Luke Mooney and Hugh Herr[2] with improvements to increase efficiency and user comfort. The device provides mechanical assistance during the stance-to-swing portion of the walking gait. It applies a torque around each ankle by pulling the ends of two struts on each foot, reducing the biological energy cost of walking.

This paper discusses the exoskeleton's mechanical and electrical design choices, and overviews preliminary control and torque simulations with the unbuilt model. It also highlights the design improvements compared to previous designs, which include more effective moment arms, a better mounting system, a more powerful motor, and a flexible design. The final exoskeleton is a sleek, modular system capable of generating torques comparable to normal biological ankle torque during walking. It is ready for manufacture and testing with novel control systems.

## 3. Methods and Results

The exoskeleton generates an ankle torque during the stance-to-swing transition phase of the walking gait using two struts attached to each foot (figure 1). The struts are attached to the inner and outer sides of the foot near the toe by a pin that allows them to rotate. This rotation is

constrained by a heel cord connecting the central part of the strut to the heel, allowing the strut to fall towards the ground under slack. Under power, the heel cord prevents the strut from rotating beyond a maximum angle, generating a torque around the ankle. The strut is actuated through a cable attached to its top part with a load cell to measure force applied (Degraw, 400 N). The motor winds the cable with a spool to pull on it. Once it reaches its maximum angle, the heel cord constrains further rotation. This motor (Maxon 305013) and its associated electronics can be located at the shin, where force is directly applied, or at the waist, where Bowden cables carry the motor force to the struts. The assembly is present on each foot, allowing separate control.

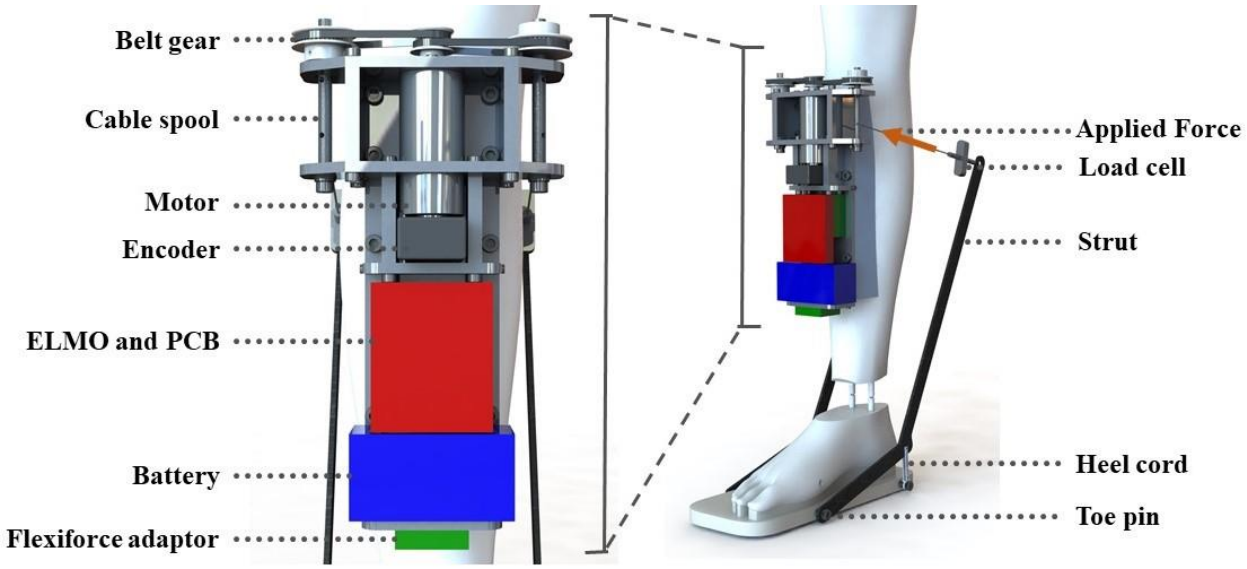


***Figure 1.*** The shin-mount exoskeleton, with parts labeled. Two large struts on either side of the leg make up the actuated moment arm. The motor, which can be mounted on the shin (as shown) or in a separate back mount, pulls on the struts to generate torque around the ankle. The device also contains various support electronics and sensors to facilitate control.

The device includes four subsystems that were mostly considered independently: struts, attachment, electronics, and control (see supplemental materials for a complete bill of materials). The strut and shoe attachment systems are dependent on the shoe size of the subject, but the remainder of the exoskeleton can be used with any adult subject. Another student, Toussaint Pegues, focused on the bodily attachment mechanisms. I worked on the remainder of the project, including the strut designs, simulations and theory to determine the exact conversion of force to torque, cable routing for different mounting locations, design of the shin and back motor mounts, control simulations in MATLAB and OpenSim, and design and assembly of the custom PCBs.

*3.1. Strut design and operation*

Several strut designs were considered based on their ability to maximize torque, minimize size, and reduce the horizontal component of the forces on the foot. The latter criterion is associated with increased user comfort during use[2].

Previous work used a straight rectangular prism as the moment arm[2], but it was not clear how this strut converted applied force into ankle torque. We modeled the strut-ankle system in a static

Solidworks simulation to gain an understanding of the physics behind its operation. The ankle was modeled as a torsion spring (stiffness $k = 100$) connected to a rigid body with the same dimensions as a typical human foot (size 13, men's). The lower end of the strut was connected to the tip of the foot and the heel cord was modeled as a rigid connection between the center of the strut and the rear end of the foot (figure 2). When a horizontal force was applied to the upper end of the strut, it caused the system to rotate by a measurable angle $\theta$. The resulting applied torque was calculated using the angular definition of torque:

$$\tau = \theta \cdot k \qquad \text{(Equation 1)}$$

The results (figure 2) were consistent with the typical definition of torque (equation 2), where $\boldsymbol{r}$ is the vector lying in the plane of the strut's outer face pointing from the toe attachment point to the force application region (figure 2). As force increased, some deviation was observed in the simulations likely due to deformation. This result was verified through similar simulations with an angled strut, since equation 2 is independent of the shape of the moment arm.

$$\boldsymbol{\tau} = \boldsymbol{r} \times \boldsymbol{F} \qquad \text{(Equation 2)}$$

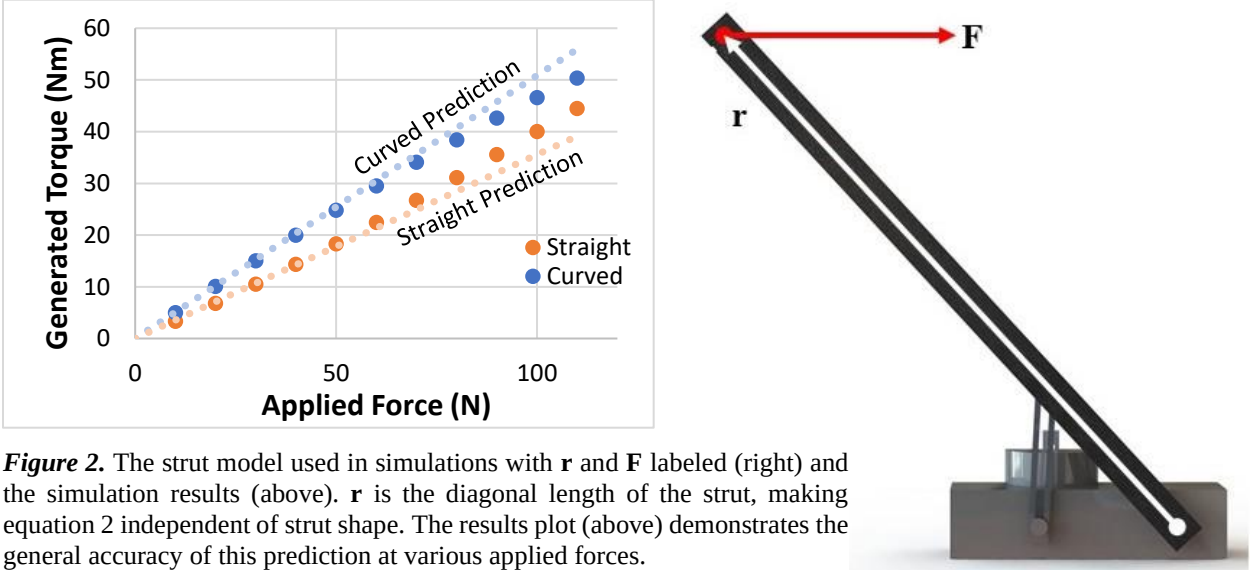


***Figure 2.*** The strut model used in simulations with **r** and **F** labeled (right) and the simulation results (above). **r** is the diagonal length of the strut, making equation 2 independent of strut shape. The results plot (above) demonstrates the general accuracy of this prediction at various applied forces.

The simulations also showed that the straight strut required a long heel cord to minimize horizontal forces on the foot. The angled strut, based on the shape of the foot-leg system, achieved the same largely vertical heel forces using a much shorter connection and without compromising torque produced. This design was used in place of the straight strut with minor modifications to ensure the strut did not touch the ground or the leg during normal walking motions. A different strut must be used depending on the subject's foot size. These tests were conducted with the men's size 11 strut. With this shoe size, the motor is capable of quickly producing torques up to 4,019 Nm (stall), with nominal torque at 118 Nm. The stall torque greatly exceeds normal biological torque, and the nominal value is just under the biological torque during normal walking for a 60 kg individual[7].

*3.2. Sensors and electronics package*

The exoskeleton requires a battery (6S LiPo), motor controller (ELMO Gold Solo Twitter), and various sensors to operate. Two printed circuit boards (PCBs) were designed to facilitate the regulation of battery voltage and the connections between the motor, encoder, motor controller, hall effect sensor, and Teensy microprocessor. The smaller PCB (2.12 x 2.6 in), for use with a single leg, supports one motor and its controller. It is designed to mount above the motor controller and uses a 1 Ah battery. A larger PCB (2.55 x 2.7 in) that supports two motors with a single battery (3 Ah) was also designed to consolidate electronics for an exoskeleton with actuators on both ankles (see supplemental materials for the complete schematics).

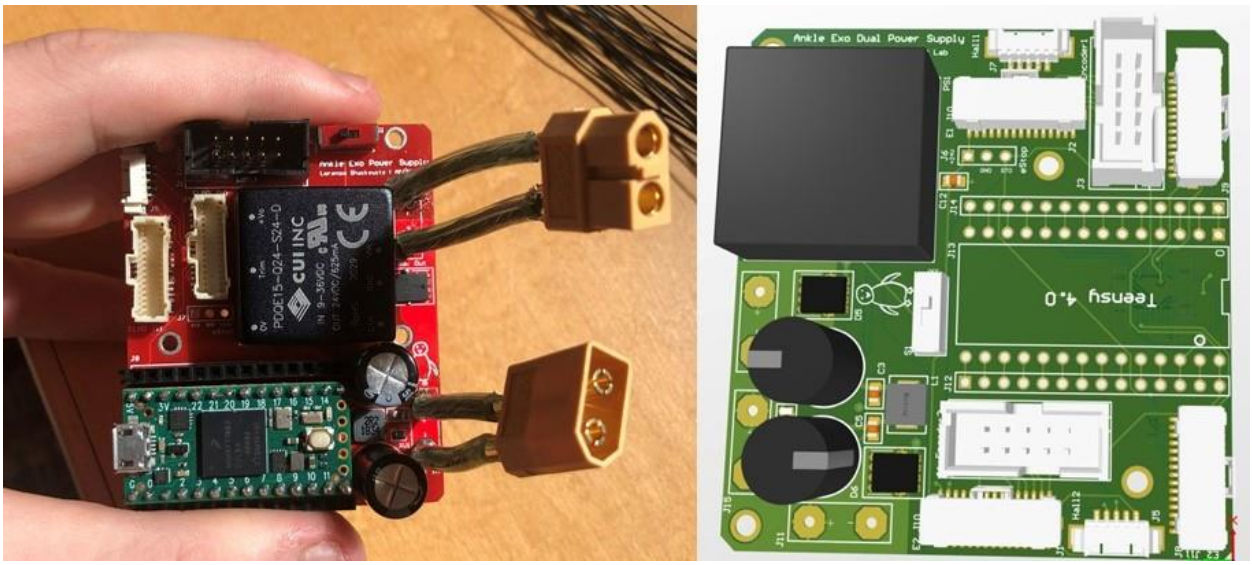


***Figure 3.*** The one-motor PCB (left) and the two-motor PCB (right). Both use a single battery (6S lipo) with regulated voltage to power the Teensy and ELMO motor controller. The two-motor board contains copies of the components that connect to the ELMO, allowing compact control of two motors.

Both PCBs break out the unused pins of the Teensy, allowing connection to external sensors. These include a footswitch (Flexiforce) embedded in the shoe and an inline load cell that senses force applied to the strut. The load cell was tested for accuracy and speed using various known masses after calibration. It operated at 52 Hz and obtained forces within 1.5% of the correct value.

*3.3. Motor mounting*

The motor mount holds the motor and its associated electronics. All electronics are clustered together to reduce extraneous wiring. The motor is attached to two spools with belt gears (gear ratio: 1.53) which wind and unwind simultaneously to apply a force to the struts. Mounting locations were considered based on their ability to reduce metabolic cost while minimizing design complexity. A shin, a knee, and a back mount were evaluated for their ease of mounting[8], contribution to moment of inertia (assuming a mass of 500 g per leg), ability to hold electronics, and difficulty of Bowden cable routing. To aid in the latter criterion, metal Bowden cable (Aircraft Spruce Co) was tested for bend capability and friction changes. Bowden cable designs corresponding to each mounting location were prototyped.

The shin mount design provides simple actuation and mounting but significantly increases the moment of inertia of the leg, reducing the overall effectiveness of the exoskeleton. However, cables can run directly from the shin mount to the struts without needing any additional attachments to ensure correct positioning, greatly simplifying routing. The back mount provides the opposite advantage: a minimal contribution to the leg's moment of inertia paired with more complicated cable routing across 2 joints of the leg.

The knee mount combines the drawbacks of the other designs without presenting many advantages. The soft and muscular nature of the upper knee makes it a difficult mounting location[8], and it still significantly contributes to moment of inertia without simplifying strut connections. Given their separate advantages, we chose to make a shin mount for quick testing and a back mount for longer-term efficiency.

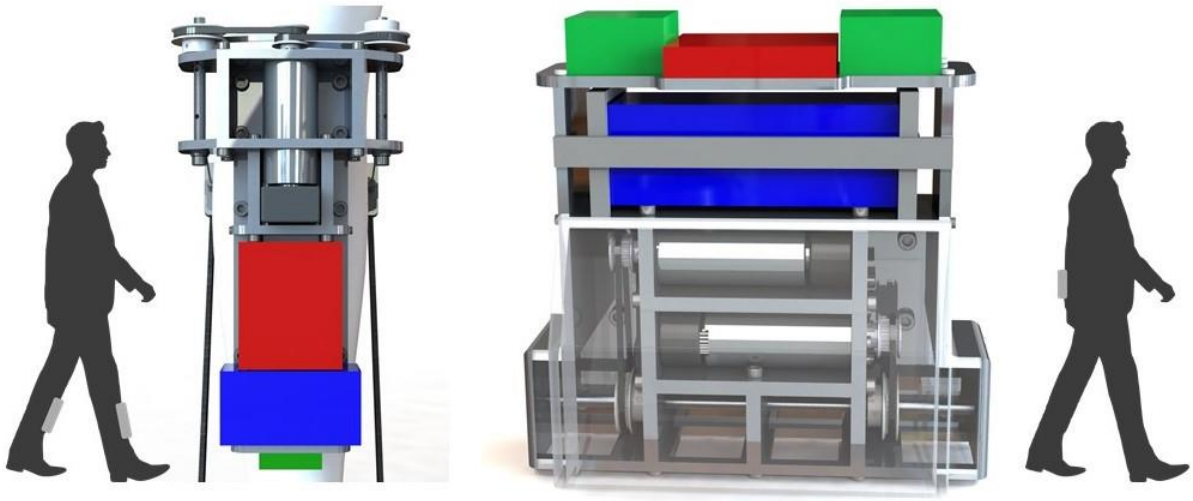

***Figure 4.*** The shin mount (left) and the back mount (right), along with their mounting locations. The exoskeleton requires two shin mounts or a single back mount to operate. While the back mount's integrated design and advantageous location minimizes mass and moment of inertia, the shin mount allows for much simpler actuation because it is right next to the struts.

The shin mount design (figures 1, 4) mounts on a modified shin guard and actuates the struts with cables that run directly from the spool to the struts. All electronics are concentrated below the motor to prevent any cables from running up the leg.

The more complex back mounted design (figure 4) concentrates the motors and electronics in a backpack. The motors are connected to the struts through cables that run down the leg. The cables run down the side of the leg, limiting their change in length as the joints they traverse rotate. The metal Bowden cable was too stiff and heavy to be used on the exoskeleton, but it did provide some useful design rules. Bowden cable needs to be held stiffly wherever it bends, and minimizing bending reduces friction. The back mount is designed to reduce the flexion of the cable by releasing it downwards.

*3.4. Device control in simulation*

To verify the efficacy of the new strut design, I constructed a simulation of a leg with two struts in Simulink. An actuator at the ankle modeled the biological torque, while actuators at the end of each strut modeled the exoskeleton's mechanical addition. Gravity was eliminated to simulate the conditions of mid-step. The biological actuator used input from experimentally derived ankle torque data[7] and feedback from an angular position sensor to maintain a total torque through time that matched a typical walking gait. Mechanical torque from the struts, limited to the clockwise (negative) direction, was applied as a force proportional to angular position and not exceeding 120 N, a safe moderate value for our motors. This allowed a direct comparison of the biological torque exerted with and without mechanical aid. In this simple system, the angular position of the foot was constantly proportionally to the total applied torque, making it an accurate torque sensor for feedback. These simulations showed the strut mechanism could completely replace biological torque at higher forces and reduce it by 68 Nm instantaneously with moderate force (figure 5).

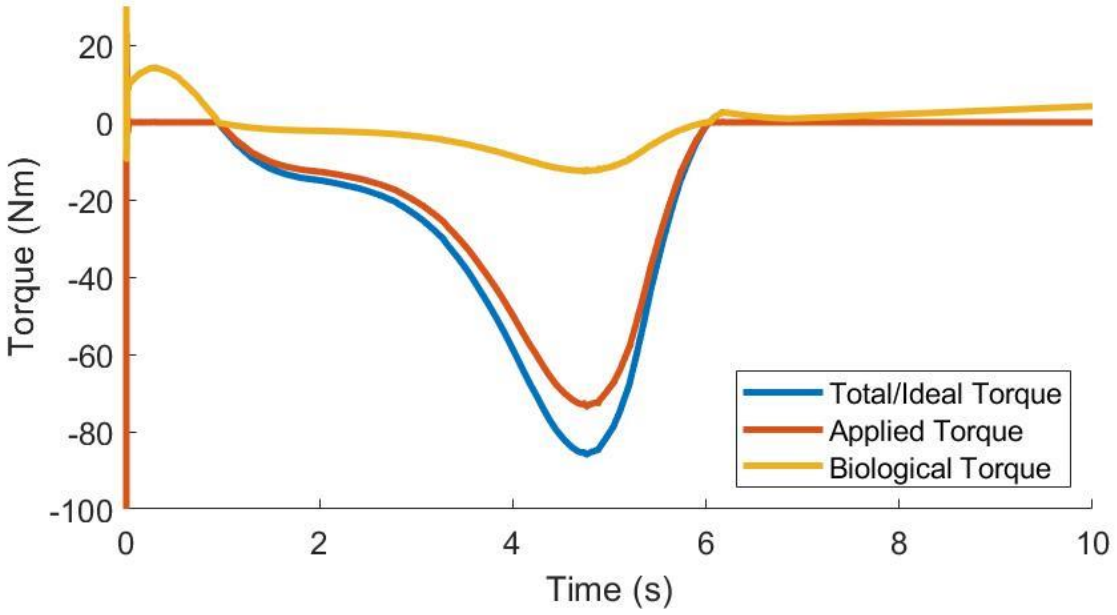


***Figure 5.*** The biological torque required to maintain a steady walking gait with only moderate exoskeleton assistance. Torque was applied in the clockwise (negative) by applying a force to the struts proportional to ankle angle but not exceeding 120 N. Under this moderate force, the struts almost completely replace biological torque.

Once designs were finalized, these limited simulations were replaced by an OpenSim[9] model of the exoskeleton in its shin mount configuration. The model was based on the Gait 2354 model and one step walking data, which removes some muscle groups for efficient simulation (see the video in supplementary materials). The model was modified to include exoskeleton struts and masses (420 g added to the foot, 600 g added to the calf). The strut force was kept parallel to the ground for simplicity and treated as an external force. Computed muscle control was used to generate muscle activation patterns for the base model and the unpowered exoskeleton. This showed the unpowered shin mounted exoskeleton increased muscle activity by an average of 4.21%.

## 4. Discussion

Early simulation results strongly suggest this exoskeleton will be capable of applying significant torques to the body. Once assembled, the device will serve as a capable platform for testing and comparing different control mechanisms. It may be used as part of a larger exoskeleton or on its own, and its modular design allows it to fit on many different subjects with electronics concentrated at the shin for convenience or at the back for efficiency.

Since the design uses a proven mechanism to actuate the ankle, the large torques calculated and observed in simulation are not surprising. The basic principle behind the conversion of force to torque (equation 2) was obtained through simulation but follows from a physical analysis of the system. The model used was purely experiencing rotational motion because it was fixed in space, so the total net force acting on it was zero. In this scenario, torque is dependent only on the points of rotation and force application; the choice of reference point makes no difference. Since the strut rotates about the toe attachment point, equation 2 gives the torque it generates. That same torque is measured at the ankle since the system's torque is independent of reference point.

In the real exoskeleton there is a nonzero net force, leading to the breakdown of this independence of reference point. However, the calculated torques closely align with values obtained experimentally using a similar exoskeleton[7], suggesting equation 2 is still mostly accurate. The expected deviations from equation 2 in the real world are different from the ones observed in simulation (figure 2). Those are related to strut deformation, which occurs differently depending on the strut's shape and increases with larger forces.

Equation 2 will be used to estimate torque generated in real time by the assembled exoskeleton with the help of a load cell. While the tested load cell is accurate, its data acquisition frequency is too slow for direct incorporation into control. The footswitch is available for use in control, but algorithms reliant on sensor data such as acceleration will need to use the broken out Teensy pins to add any other required sensors. This breakout space increases the modularity of the system, ensuring it can be adapted for many different control frameworks.

The basic control simulation performed (figure 5) is more useful as a comparison of exoskeleton torque and biological torque than as a plan for control. Without muscles or walking motion modeled, the Simulink model doesn't predict how muscles will respond to the application of torque and cannot quantify the energy tradeoff between added mass and exoskeleton assistance since gravity is not considered. This set of simplifications suggests more complex models like OpenSim and experimental results should not expect large reductions in metabolic activity due to exoskeleton power. However, other work on a similar ankle exoskeleton has shown the ankle angle-based control we employed is an effective method in human trials[2].

### *4.1.Future work*

This project still needs significant prototyping and a basic control framework. The two mounting locations need to be machined and assembled, with design changes considered based on simple physical tests. The electronics, including the PCB, need to be connected and tested with load applied to the motor. The Teensy lacks a programmable framework to simplify connection to the motor and allow simple incorporation of different control algorithms. Finally, a reliable set of controls should be developed with the OpenSim model to compare with results from human

subjects. Once the exoskeleton is built, programmed, and tested, it will be able to serve as a robust platform for further controls testing.

## 5. References


1. Esquenazi, A., Talaty, M., Packel, A. & Saulino, M. The ReWalk Powered Exoskeleton to Restore Ambulatory Function to Individuals with Thoracic-Level Motor-Complete Spinal Cord Injury. *American Journal of Physical Medicine & Rehabilitation* **91**, (2012).
2. Mooney, L. M., Rouse, E. J. & Herr, H. M. Autonomous exoskeleton reduces metabolic cost of human walking during load carriage. *Journal of NeuroEngineering and Rehabilitation* **11**, 80 (2014).
3. Mooney, L. M., Rouse, E. J. & Herr, H. M. Autonomous exoskeleton reduces metabolic cost of human walking. *Journal of NeuroEngineering and Rehabilitation* **11**, 151 (2014).
4. Collins, S. H., Wiggin, M. B. & Sawicki, G. S. Reducing the energy cost of human walking using an unpowered exoskeleton. *Nature* **522**, 212–215 (2015).
5. Young, A. J., Gannon, H. & Ferris, D. P. A Biomechanical Comparison of Proportional Electromyography Control to Biological Torque Control Using a Powered Hip Exoskeleton. *Frontiers in Bioengineering and Biotechnology* **5**, 37 (2017).
6. Galle, S., Malcolm, P., Collins, S. H. & De Clercq, D. Reducing the metabolic cost of walking with an ankle exoskeleton: interaction between actuation timing and power. *Journal of NeuroEngineering and Rehabilitation* **14**, 35 (2017).
7. Mooney, L. M. & Herr, H. M. Biomechanical walking mechanisms underlying the metabolic reduction caused by an autonomous exoskeleton. *Journal of NeuroEngineering and Rehabilitation* **13**, 4 (2016).
8. Witte, K. A. & Collins, S. H. Design of lower-limb exoskeletons and emulator systems. in *Design of lower-limb exoskeletons and emulator systems* 251–274 (Wearable Robotics: Systems and Applications, 2019).
9. Seth, A. *et al.* OpenSim: Simulating musculoskeletal dynamics and neuromuscular control to study human and animal movement. *PLOS Computational Biology* **14**, e1006223 (2018).


## 6. Acknowledgements


I thank Maegan Tucker for guiding me through this project and Dr. Aaron Ames for providing the resources that made this possible. I also acknowledge Toussaint Pegues for his assistance throughout the project. This work was supported by the Student-Faculty Programs office and SURF.


## 7. Supplemental Materials

A bill of materials, video of the OpenSim model, and PCB schematics can be found at https://lorenzos.me/projects/ankle-exo.